Supporting Information

Nie et al. 10.1073/pnas.1406019111

SI Text

Lattice Model

To provide an explicit UV cutoff for integrals in a way that is guaranteed to respect the underlying lattice symmetries, we have defined a lattice version of the Hamiltonian (Eq. **6** in the main text), which we have used when obtaining explicit numerical solutions of the model,

$$\begin{aligned}H=&-J\sum_{\langle\vec{r},\vec{r}'\rangle}\sum_{m}\left[\psi^{\dagger}(\vec{r},m)\psi(\vec{r}',m)+\text{C.C.}\right]\\&-J'\sum_{\vec{r},m}\Big[\psi^{\dagger}(\vec{r},m)\tau\psi(\vec{r}+\hat{x},m)\\&-\psi^{\dagger}(\vec{r},m)\tau\psi(\vec{r}+\hat{y},m)+\text{C.C.}\Big]\\&+\frac{U}{2N}\sum_{\vec{r},m}\left[\psi^{\dagger}(\vec{r},m)\psi(\vec{r},m)-N\Lambda\right]^2\\&-\frac{\Delta}{2N}\sum_{\vec{r},m}\left[\psi^{\dagger}(\vec{r},m)\tau\psi(\vec{r},m)\right]^2\\&-V_z\sum_{\vec{r},m}\left[\psi^{\dagger}(\vec{r},m)\psi(\vec{r},m+1)+\text{C.C.}\right]\\&-\sum_{\vec{r},m}\left[h^{\dagger}(\vec{r},m)\psi(\vec{r},m)+\text{C.C.}\right],\end{aligned}\qquad[\text{S1}]$$

where $\psi_{\alpha,j}$ is a two-index $2\times N$ component field, where $\alpha=x,y$ refers to the direction of the charge density wave (CDW) and J and J' are related to the transverse and longitudinal stiffnesses in the field theory according to

$$J=\frac{1}{2}(\kappa_{\parallel}+\kappa_{\perp}),\quad J'=\frac{1}{2}(\kappa_{\parallel}-\kappa_{\perp}),\quad \tau=\begin{pmatrix}\mathbb{I}_{N\times N} & \\ & -\mathbb{I}_{N\times N}\end{pmatrix}.\qquad[\text{S2}]$$

The vector $\vec{r}$ denotes the position in a given layer (x,y plane) and m labels the layers (z axis). When there is no ambiguity, we use the notation $\mathbf{r}\equiv(\vec{r},m)$ in the following. The Z_2 symmetry of the model under $x\to y$, $y\to -x$, and $\psi_{x,j}\to\psi_{y,j}$ and $\psi_{y,j}\to-\psi_{x,j}$ represents the C_4 symmetry of the physical system, whereas the $SO(N)$ rotational symmetry represents a generalized translational symmetry. [In the physical $O(2)$ case, the two components of $\psi_{\alpha,j}$ correspond to the real and imaginary parts of the complex CDW amplitude, ψ_{α} defined in Eq. **1** of the main text.]

Henceforth, we consider the model in the limit $U\to\infty$, where the term proportional to U is omitted and instead ψ is subjected to the hard-spin constraint, $\psi^{\dagger}\psi=N\Lambda$, which we enforce by introducing the Lagrange-multiplier field $\zeta(\mathbf{r})$. We also perform a Hubbard–Stratonovich transformation that introduces the nematic field $\phi(\mathbf{r})$ to replace the quartic term Δ. The Hamiltonian then reads

$$\begin{aligned}H[\psi,\phi,\mu,h]=&-J\sum_{\langle\vec{r},\vec{r}'\rangle}\sum_{m}\left[\psi^{\dagger}(\vec{r},m)\psi(\vec{r}',m)+\text{C.C.}\right]\\&-J'\sum_{\mathbf{r}}\left[\psi^{\dagger}(\mathbf{r})\tau\psi(\mathbf{r}+\hat{x})-\psi^{\dagger}(\mathbf{r})\tau\psi(\mathbf{r}+\hat{y})+\text{C.C.}\right]\\&+i\sum_{\mathbf{r}}\zeta(\mathbf{r})\left[\psi^{\dagger}(\mathbf{r})\psi(\mathbf{r})-N\Lambda\right]\\&+\frac{1}{\sqrt{N}}\sum_{\mathbf{r}}\phi(\mathbf{r})\left[\psi^{\dagger}(\mathbf{r})\tau\psi(\mathbf{r})\right]+\frac{1}{2\Delta}\sum_{\mathbf{r}}\phi^2(\mathbf{r})\\&-V_z\sum_{\vec{r},m}\left[\psi^{\dagger}(\vec{r},m)\psi(\vec{r},m+1)+\text{C.C.}\right]\\&-\sum_{\mathbf{r}}\left[h^{\dagger}(\mathbf{r})\psi(\mathbf{r})+\text{C.C.}\right].\end{aligned}\qquad[\text{S3}]$$

Replicas and the Configuration Average

To better exhibit the statistical symmetries of the model, we introduce n replicas of the system. This allows us to define an effective, translationally invariant model in which the averages over the random fields have been explicitly performed,

$$\exp\left(-\beta H_{\text{rep}}\left[\left\{\psi^{(a)},\phi^{(a)},\zeta^{(a)}\right\}\right]\right)\equiv\overline{\exp\left(-\sum_{a=1}^{n}H\left[\psi^{(a)},\phi^{(a)},\zeta^{(a)};h\right]\right)},\qquad[\text{S4}]$$

where $h_{\alpha j}$ are Gaussian random variables with

$$\overline{h_{\alpha j}(\mathbf{r})}=0,\qquad\overline{h_{\alpha j}(\mathbf{r})h_{\alpha' j'}(\mathbf{r}')}=\sigma^2\delta_{\alpha,\alpha'}\delta_{j,j'}\delta_{\vec{r},\vec{r}'}\delta_{m,m'},\qquad[\text{S5}]$$

and hence

$$\begin{aligned}H_{\text{rep}}\left[\left\{\psi^{(a)},\phi^{(a)},\zeta^{(a)}\right\}\right]=&\sum_{a}H\left[\psi^{(a)},\phi^{(a)},\zeta^{(a)};0\right]\\&-\frac{\beta\sigma^2}{2}\sum_{a,a'}\sum_{\mathbf{r}}\left[\psi^{(a)\dagger}(\mathbf{r})\psi^{(a')}(\mathbf{r})+\text{C.C.}\right].\end{aligned}\qquad[\text{S6}]$$

To focus on the nematic order parameter itself, we formally define the effective Hamiltonian expressed in terms of the replica nematic fields $\phi^{(a)}$ alone by integrating out the remaining fields,

$$\begin{aligned}&\exp\left(-\beta H_{\text{eff}}\left[\left\{\phi^{(a)}\right\}\right]\right)\\&\quad\equiv\int\prod_{a=1}^{n}d\zeta^{(a)}\mathcal{D}\psi^{(a)}\exp\left(-\beta H_{\text{rep}}\left[\left\{\psi^{(a)},\phi^{(a)},\zeta^{(a)}\right\}\right]\right).\end{aligned}\qquad[\text{S7}]$$

Because of the Yukawa-like coupling between ζ and ψ, this formal process cannot be implemented exactly. However, we can evaluate the ζ integral in saddle-point approximation, which is exact in the large N limit; this is equivalent to replacing the hard-spin constraint by the mean "spherical" constraint

$$\left\langle\psi^{(a)\dagger}(\mathbf{r})\psi^{(a)}(\mathbf{r})\right\rangle=\Lambda N,\qquad[\text{S8}]$$

which serves as an implicit equation for the saddle-point values of $\zeta^{(a)}(\mathbf{r}) = -i(\mu_a + 2J + V_z)$, where μ_a is a constant in space. Now, the integral over the CDW fields, $\psi^{(a)}$, is straightforward, because they are Gaussian and always massive,

$$H_{\text{eff}}\left[\left\{\phi^{(a)}\right\}\right] = \frac{1}{2\Delta}\sum_a\sum_{\mathbf{r}}\phi^{(a)}(\mathbf{r})^2 - N\Lambda\sum_a\sum_{\mathbf{r}}(\mu_a + 2J + V_z) \quad \textbf{[S9]}$$

$$\tilde{\mathcal{G}}^{-1}_{a\mathbf{r},a'\mathbf{r}'}\left[\left\{\phi^{(b)}\right\};\pm\right] = \left[\tilde{G}^{-1}_{\mathbf{r},\mathbf{r}'}(\mu_a;\pm) \pm \frac{\phi^{(a)}(\mathbf{r})}{\sqrt{N}}\delta_{\mathbf{r},\mathbf{r}'}\right]\delta_{a,a'} - \beta\sigma^2 \;\; \delta_{\mathbf{r},\mathbf{r}'}, \quad \textbf{[S10]}$$

where we have used the notation $\{\phi^{(b)}\}$ to stress that $\tilde{\mathcal{G}}^{-1}_{a,a'}$ depends on all replica fields (this is also true for μ_a, which depends on all $\{\phi^{(b)}\}$ s through the mean spherical condition). Furthermore,

$$\tilde{G}^{-1}_{\mathbf{r},\mathbf{r}'}(\mu;\pm) = -\frac{(J \pm J')}{2}\left[\delta_{\mathbf{r}-\mathbf{r}',\hat{x}} + \delta_{\mathbf{r}-\mathbf{r}',-\hat{x}}\right] + -\frac{(J \mp J')}{2}\left[\delta_{\mathbf{r}-\mathbf{r}',\hat{y}} + \delta_{\mathbf{r}-\mathbf{r}',-\hat{y}}\right] - \frac{V_z}{2}\left[\delta_{\mathbf{r}-\mathbf{r}',\hat{z}} + \delta_{\mathbf{r}-\mathbf{r}',-\hat{z}}\right] + (\mu + 2J + V_z)\delta_{\mathbf{r},\mathbf{r}'}. \quad \textbf{[S11]}$$

Exploiting the translational symmetry of the replicated model, we can obtain the Fourier transform of $\tilde{G}$,

$$G(\mathbf{k};\mu;\pm)^{-1} = 2(J \pm J')\sin^2\frac{k_x}{2} + 2(J \mp J')\sin^2\frac{k_x}{2} + 2V_z\sin^2(k_z) + \mu, \quad \textbf{[S12]}$$

where G is the lattice version of the corresponding quantity defined in Eq. **3** of the main text.

The formal expression for H_{eff} is generally extremely complicated. It can be expanded in increasing number of sums over replicas to generate a cumulant expansion (1) and can further be expanded in gradients of the fields $\phi^{(a)}$, assuming that the latter are slowly varying in space. In the case where we completely neglect the spatial variation of $\phi^{(a)}$, we can define $\mathcal{N}_a \equiv \phi^{(a)}/\sqrt{N}$, and $\tilde{\mathcal{G}}$ can be diagonalized by Fourier transform, yielding

$$\mathcal{G}_{aa'}\left(\mathbf{k};\{\mathcal{N}_b\};\pm\right) = G\left(\mathbf{k};\mu_a \pm \mathcal{N}_a;\pm\right)\delta_{a,a'} + \beta\sigma^2\frac{G\left(\mathbf{k};\mu_a \pm \mathcal{N}_a;\pm\right)G\left(\mathbf{k};\mu_{a'} \pm \mathcal{N}_{a'};\pm\right)}{1 - \beta\sigma^2\sum_b G\left(\mathbf{k};\mu_b \pm \mathcal{N}_b;\pm\right)}. \quad \textbf{[S13]}$$

Under these circumstances,

$$H_{\text{eff}}\left[\left\{\sqrt{N}\mathcal{N}_a\right\}\right] = V\left\{\sum_a\left[\frac{\mathcal{N}_a^2}{2\Delta} - \Lambda(\mu_a + 2J + V_z)\right] - \frac{T}{2}\sum_{\alpha=\pm}\int\frac{d^3k}{(2\pi)^3}\text{Tr}\left\{\ln\left(T\mathcal{G}\left[\mathbf{k};\{\mathcal{N}_a\};\alpha\right]\right)\right\}\right\}, \quad \textbf{[S14]}$$

where $V = \sum_{\vec{r}}1$ is the volume and the trace, now, is only over the replica index. After expanding in increasing number of sums over replicas, we obtain

$$\frac{H_{\text{eff}}\left[\left\{\sqrt{N}\mathcal{N}_a\right\}\right]}{NV} = \sum_a\left\{\frac{\mathcal{N}_a^2}{2\Delta} - \Lambda\left(\mu\left[\mathcal{N}_a\right] + 2J + V_z\right) - \frac{T}{2}\sum_{\alpha=\pm}\int\frac{d^3k}{(2\pi)^3} \times\left[\ln\left(TG\left(\mathbf{k};\mathcal{N}_a;\alpha\right)\right) + \beta\sigma^2 G\left(\mathbf{k};\mathcal{N}_a;\alpha\right)\right]\right\} - \frac{\beta\sigma^4}{4}\sum_{a,a'}\sum_{\alpha=\pm}\int\frac{d^3k}{(2\pi)^3}G\left(\mathbf{k};\mathcal{N}_a;\alpha\right)G\left(\mathbf{k};\mathcal{N}_{a'};\alpha\right) + \mathcal{O}\left(\sum_{a,a',a''}\right), \quad \textbf{[S15]}$$

where we have defined for convenience $G(\mathbf{k};\mathcal{N}_a;\pm) \equiv G(\mathbf{k};\mu[\mathcal{N}_a] \pm \mathcal{N}_a;\pm)$ and $\mu[\mathcal{N}_a]$ is the solution of the saddle-point equation at the lowest order in the number of sums over replicas:

$$\Lambda = T\sum_{\alpha=\pm}\int\frac{d^3k}{(2\pi)^3}\left[G\left(\mathbf{k};\mathcal{N}_a;\alpha\right) + \sigma^2 G\left(\mathbf{k};\mathcal{N}_a;\alpha\right)^2\right]. \quad \textbf{[S16]}$$

Note that when all replica nematic fields are equal, $\mathcal{N}_a = \mathcal{N}$, the above expansion in Eq. **S15** is equivalent to an expansion in powers of the number of replicas n and one recovers the standard replica trick when $n \to 0$.

The replicated theory makes manifest the statistical symmetries of the problem. Clearly, H_{eff} in Eq. **S9** is translationally invariant. However, the index $\pm$ in $\tilde{G}$ brings on an explicit dependence on spatial orientation; for + the preferred axis is in the x direction and for − it is in the y direction. Thus, H_{eff} has a sort of "spin-orbit coupling," such that it is not invariant under C_4 spatial rotation or any transformation of the order parameter alone. Moreover, because of the coupling between different replicas generated by the σ-dependent terms, no transformation that acts on a subset of replicas leaves H_{eff} invariant; this is the property that identifies the problem as a random-field problem. H_{eff} is invariant under the discrete rotation $\phi^{(a)}(\vec{r},m) \to -\phi^{(a)}(\vec{r}',m)$ with $x' = y$ and $y' = -x$. This is the symmetry that identifies the problem as a version of the Ising model. [The model is also invariant under the mirror-plane transformation $\phi^{(a)}(\vec{r},m) \to -\phi^{(a)}(\vec{r}',m)$ with $x' = y$ and $y' = x$.]

Relation to the Random-Field Ising Model

To establish the relation between H_{eff} and the random-field Ising Model (RFIM), we perform the same sort of analysis for the RFIM. We start with a general Ising ferromagnet in a random field,

$$\beta H_{\text{RFIM}}[S] = -\frac{1}{2}\sum_{ij}S_i K_{ij} S_j - \beta\sum_i H_i S_i, \quad \textbf{[S17]}$$

where $S_i = \pm 1$, $K_{ij} \geq 0$, and H_j is a Gaussian random variable with zero mean. This can be recast in terms of real scalar fields Φ_i by a series of transformations discussed in ref. 2 as

$$\beta\tilde{H}_{\text{RFIM}}[\Phi] = \frac{1}{2}\sum_{ij}\Phi_i K_{ij}\Phi_j - \sum_i\ln\left[\cosh\left(\sum_j 2K_{ij}\Phi_j\right)\right] - \beta\sum_i H_i\Phi_i + \frac{\beta^2}{2}\sum_{ij}H_i K_{ij}^{-1}H_j. \quad \textbf{[S18]}$$

Here, the first two terms represent the effective Hamiltonian of the pure Ising ferromagnet, and the final term can be

viewed as a correction to the random-field distribution. Just as we did for the CDW model, we introduce n replicas of the Ising fields and then perform the average over the random variables, resulting in

$$\beta H^{\rm eff}_{\rm RFIM}\left[\left\{\Phi^{(a)}\right\}\right] = \sum_a \left\{ \sum_{ij} \frac{1}{2}\Phi_i^{(a)} K_{ij} \Phi_j^{(a)} - \sum_i \ln\left[\cosh\left(\sum_j 2K_{ij}\Phi_j^{(a)}\right)\right]\right\} - \frac{\beta^2}{2}\sum_{a,a'}\sum_{ij}\Phi_i^{(a)} D_{ij} \Phi_j^{(a')}, \quad \textbf{[S19]}$$

where

$$D_{ij} = \overline{H_i H_j} \quad \textbf{[S20]}$$

with the average performed over an ensemble that includes the effect of the final term in Eq. **S18**.

The symmetries of this problem are manifestly similar to those of $H_{\rm eff}$. Again, there is no symmetry under transformations that involve a subset of the replicas. Indeed, $H^{\rm eff}_{\rm RFIM}$ is invariant under all of the same transformations as $H_{\rm eff}$, but because the RFIM as defined has no spin-orbit coupling, it has an additional invariance with respect to pure spatial transformations of the type $\Phi^{(a)}(\mathbf{r}) \to \Phi^{(a)}(\mathbf{r}')$.

An explicit correspondence between the two models can be made in different fashions in different parameter regimes (compare, for instance, Eqs. **S15** and **S19** when the field Φ is uniform). For T near to the nematic ordering temperature, the effective Hamiltonian can be expanded in powers of the order parameter fields and their spatial derivatives and can be compared term by term. To illustrate the point, we consider the terms in $H_{\rm eff}$ to zeroth order in spatial derivatives [i.e., evaluated for constant values of $\phi^{(a)} = \sqrt{N}\,\mathcal{N}_a$]. From Eq. **S15** one easily derives

$$\beta H_{\rm eff} = \sum_{\mathbf{r}} \left\{ \sum_a \left[\frac{B_1}{2}\mathcal{N}_a^2 + \frac{C_1}{4!}\mathcal{N}_a^4\right] - \frac{1}{2}\sum_{a,a'}\left[B_2 \mathcal{N}_a \mathcal{N}_{a'} + C_2 \mathcal{N}_a^2 \mathcal{N}_{a'}^2\right] + \frac{1}{3!}\sum_{a,a',a''} C_3 \mathcal{N}_a \mathcal{N}_{a'} \mathcal{N}_{a''}^2 \right\} + \ldots, \quad \textbf{[S21]}$$

where ... indicates higher powers of the field and their derivatives and

$$\frac{B_1}{N} = -\mu_0''\left(\beta\Lambda - \frac{1}{2}\sum_{\alpha=\pm}\int_k \left[G(\mathbf{k};\mu_0;\alpha) + \sigma^2 G(\mathbf{k};\mu_0;\alpha)^2\right]\right) - \sum_{\alpha=\pm}\int_k \left[G(\mathbf{k};\mu_0;\alpha)^2 + \sigma^2 G(\mathbf{k};\mu_0;\alpha)^3\right] + \frac{\beta}{\Delta},$$

$$\frac{B_2}{N} = \frac{\beta^2\sigma^4}{2}\sum_{\alpha=\pm}\int_k G(\mathbf{k};\mu_0;\alpha)^4,$$

$$\frac{C_2}{N} = 2\beta^2\sigma^4\sum_{\alpha=\pm}\int_k G(\mathbf{k};\mu_0;\alpha)^6, \quad \textbf{[S22]}$$

where μ_0 is the solution of Eq. **S16** when $\mathcal{N} = 0$ and $\mu_0'' = \partial^2\mu/\partial\mathcal{N}^2|_{\mathcal{N}=0}$. Moreover, $C_3 \neq 0$ when $\sigma^2 > 0$.

The corresponding expression for $H^{\rm eff}_{\rm RFIM}$ is of the same form, but with parameters

$$\begin{aligned} B_1' &= K(1-2K) = \beta T_{\rm MF}(1-\beta T_{\rm MF}), \\ B_2' &= \beta^2 D, \\ C_2' &= C_3' = \cdots = 0, \end{aligned} \quad \textbf{[S23]}$$

where

$$K \equiv \sum_j K_{ij} \equiv \frac{\beta T_{\rm MF}}{2}, \quad \text{and} \quad D \equiv \sum_j D_{ij}. \quad \textbf{[S24]}$$

The expression of the other terms can be similarly obtained but is not particularly illuminating and is not given here.

There are some manifest, but ultimately unimportant differences in the structure of the two models. First, $C_p = 0$ for all $p > 1$ in the standard RFIM. This is an artifact of the simple version of the model assumed; random bond disorder (randomness in the values of K_{ij}) would immediately generate a nonzero C_2 and a non-Gaussian distribution of the random fields as well as a combination of both random bonds and random fields, resulting in nonzero values for the other coefficients. These terms are irrelevant for universal physics at a large scale. A more subtle issue is that B_1' is independent of the disorder in the RFIM, whereas its counterpart depends implicitly on σ for the CDW system; again, this is a peculiarity of the simple version of the RFIM considered, and the generic behavior (exhibited by the CDW model) would be generated by an imperfectly Gaussian distribution of random fields. Whereas B_1 and B_1' both change sign at a nonzero mean-field transition temperature, $T_{\rm MF}$, the T dependence of B_1' is much more complex than that of B_1; to make a precise correspondence between the models, the coupling constants entering the RFIM would have to be T and σ dependent.

It is also possible to directly compare the two effective models in the limit $T \to 0$, with results analogous to those given above, but we do not expand on this aspect here.

Despite the complexity that accompanies any attempt to establish a precise mapping between the two models, it is clear that the structure of the two models is sufficiently similar that one can adopt known results for the RFIM qualitatively and even semiquantitatively for the CDW system.

In the following sections we treat the nematic order parameter in the saddle-point approximation as a way to illustrate our conclusions by concrete results. This is entirely analogous to treating the effective field theory for the RFIM at the same level of approximation and could be replaced by more sophisticated treatments.

For the most part, the saddle-point solutions produce results that are qualitatively correct. Of course (as we shall see) they produce mean-field exponents for various critical properties, where nontrivial exponents would be expected in a more accurate treatment. Moreover, nowhere does the mean-field theory addresses the physics of rare events ("droplets") that lead to the extreme dynamical slowing down that is characteristic of the RFIM.

However, the most important failure of the mean-field treatment occurs in the $d = 2$ limit, $V_z = 0$, where there is a particular subtlety associated with the formation of Imry–Ma domains—whereas the saddle-point equations admit a nematic phase at weak enough disorder in 2D, the correspondence with the RFIM implies that instead there should always be a finite nematic correlation length that in the weak disorder limit is exponentially long,

$$\ln\left[\xi_{\rm 2D}\right] \sim \left(\frac{\kappa}{\sigma^{\rm eff}}\right)^2, \quad \textbf{[S25]}$$

where $\xi_{\rm 2D}$ is the correlation length of the 2D RFIM with a random field of rms magnitude $\sigma^{\rm eff} \sim \sigma^2/J$. This subtlety, however, is

less alarming than it seems at first, as it is eliminated by even extremely weak 3D couplings. To make an estimate of the way in which nonzero V_z eliminates this 2D peculiarity, we estimate a length scale associated with small nonzero V_z in the following manner: Consider a block of $L\times L$ spins in a given plane and treat them as a single, block spin. The effective coupling between block spins within a plane is JL, whereas the effective coupling between planes is V_zL^2, so for blocks of size $L=J/V_z$, the couplings become effectively isotropic, and 2D physics is no longer pertinent. Thus, the physics of 2D Imry–Ma domains are negligible as long as $V_z > J/\xi_{2D}$.

Mean-Field Solution

Saddle-Point Equations. We now turn to the saddle-point, or mean-field solution of the problem. For each replica, $\mu^{(a)}$ is determined by the mean-spherical constraint, Eq. **S8**,

$$\Lambda=\frac{T}{V}\sum_{\mathbf{r}}\left\{\tilde{\mathcal{G}}_{\mathbf{r}a,\mathbf{r}a}\left[\left\{\phi^{(b)}\right\};-\right]+\tilde{\mathcal{G}}_{\mathbf{r}a,\mathbf{r}a}\left[\left\{\phi^{(b)}\right\};+\right]\right\}, \qquad \text{[S26]}$$

whereas the saddle-point equations for the replicated field theory are given by

$$\phi^{(a)}(\mathbf{r})=T\Delta\sqrt{N}\left\{\tilde{\mathcal{G}}_{\mathbf{r}a,\mathbf{r}a}\left[\left\{\phi^{(b)}\right\};-\right]-\tilde{\mathcal{G}}_{\mathbf{r}a,\mathbf{r}a}\left[\left\{\phi^{(b)}\right\};+\right]\right\} \qquad \text{[S27]}$$

with $\tilde{\mathcal{G}}$ obtained from Eq. **S10**. Note that the symmetry-preserving state, $\phi^{(a)}=0$, is always a solution of the set of Eqs. **S26** and **S27**.

There is no proof that the nontrivial solutions of these equations with lowest free energy are always homogeneous, but we restrict ourselves to this case. Then, as before, defining $\mathcal{N}_a\equiv\phi^{(a)}/\sqrt{N}$, we can cancel the N dependence of these equations (making the $N\to\infty$ limit trivial to obtain, if we so desire). We are interested in the solution at the lowest order in the number of sums over replicas or equivalently in the limit $n\to 0$ (see above). In this case the saddle-point equations become

$$\begin{aligned}\Lambda=&T\left[A_1(\mu_a-\mathcal{N}_a)+A_1(\mu_a+\mathcal{N}_a)\right]\\&+\sigma^2\left[A_2(\mu_a-\mathcal{N}_a)+A_2(\mu_a+\mathcal{N}_a)\right],\end{aligned} \qquad \text{[S28]}$$

$$\begin{aligned}\frac{\mathcal{N}_a}{\Delta}=&T\left[A_1(\mu_a-\mathcal{N}_a)-A_1(\mu_a+\mathcal{N}_a)\right]\\&+\sigma^2\left[A_2(\mu_a-\mathcal{N}_a)-A_2(\mu_a+\mathcal{N}_a)\right],\end{aligned} \qquad \text{[S29]}$$

where $\mu_a\equiv\mu\left[\mathcal{N}_a\right]$ (Eq. **S16**) and

$$A_p(\mu)=\int\frac{d^3k}{(2\pi)^3}G(\mathbf{k};\mu;\pm)G(\mathbf{k};\mu;\pm)^{p-1} \qquad \text{[S30]}$$

with G given in Eq. **S12**. These equations are of precisely the same form as the saddle-point equations given in Eqs. **9** and **10** of the main text, with the lattice propagator G instead of the continuum propagator in the definition of A_p. The latter difference is convenient for numerical studies, as no artificial cutoff needs to be introduced to perform the integrals (which are carried out for $\mathbf{k}$ in the first Brillouin zone). Note that because of the integral over all $\mathbf{k}$, A_p does not depend on the index $\pm$. There is a separate, identical saddle-point equation for each value of the replica index, a, and, as is known from the mean-field solution of the RFIM, no exotic spontaneous replica symmetry breaking is to be expected in this case. In the remainder of this section, we explore the solutions of these saddle-point equations.

Mean-Field Phase Diagram. The mean-field phase diagrams shown in Fig. 1 in the main text and below are obtained by solving the saddle-point (mean-field) equations numerically in the $n\to 0$ limit (or, equivalently, in the replica symmetric case). The most general form of these equation is

$$\begin{aligned}\Lambda=&|\Gamma|^2+T\left[A_1(\mu-\mathcal{N})+A_1(\mu+\mathcal{N})\right]\\&+\sigma^2\left[A_2(\mu-\mathcal{N})+A_2(\mu+\mathcal{N})\right],\\\mathcal{N}/\Delta=&|\Gamma|^2+T\left[A_1(\mu-\mathcal{N})-A_1(\mu+\mathcal{N})\right]\\&+\sigma^2\left[A_2(\mu-\mathcal{N})-A_2(\mu+\mathcal{N})\right]+b^{\text{eff}},\end{aligned} \qquad \text{[S31]}$$

where $\Gamma=\overline{\langle\psi_x\rangle}$ is the magnitude of the CDW condensate (where we are still assuming that $\overline{\langle\psi_y\rangle}=0$), and b^{eff} is a possible external symmetry-breaking field (orthorhombicity) that (when positive) favors the nematic principle axis in the x direction (positive $\mathcal{N}$). Unless otherwise stated, we always assume that the crystal has tetragonal symmetry, so $b^{\text{eff}}=0$ and nematicity arises solely as a consequence of spontaneous symmetry breaking.

Clean Limit $\sigma=0$

In all of the discussion in the main text, we have always assumed $\Gamma=0$, as it must be for $\sigma>0$ in $d\le 4$. To confirm this, note that the spectrum of excitations about the saddle point is given by Eq. **S12**. Because any phase with $\Gamma\neq 0$ breaks a continuous symmetry, it must have a Goldstone mode; thus, any phase with a nonzero value of Γ must have $\mu-|\mathcal{N}|=0$. However, for σ^2, this results in a divergent value of A_2 (in $d\le 4$) and hence a violation of the hard-spin constraint. This reflects the absence of continuous symmetry breaking in the presence of quenched randomness.

However, when we compute the phase diagram in the clean limit shown in Fig. S1, we must include a nonvanishing Γ at all temperatures below T_{str}. The continuous phase transitions in this diagram are straightforward to obtain directly from the self-consistency equations; however, there are generally two distinct solutions to these equations in the vicinity of the first-order portions of the phase boundaries. Thus, to determine the location of these boundaries, it is necessary to compute the Feynman variational free energy corresponding to each solution and then favor the one with the lower free energy. For small enough V_z (i.e., for $V_z<0.38J$ in the case we have studied numerically, with $J'=0.01J$ and $\Delta=0.25J$), all of the transitions are continuous, but for V_z larger than a critical value at which there is a tricritical point, the stripe transition becomes first order.

Phase Diagram with Disorder

A nonzero nematic order parameter is possible, even with quenched randomness, for $d>2$. Indeed, it is straightforward to see from Eqs. **S28** and **S29** that at any temperature for which there is a nonzero value of the nematic order parameter at $\sigma=0$, there will still be a nonzero solution for small enough nonzero σ. The proof of this assertion is particularly simple for $T_{\text{nem}}>T>T_{\text{str}}$, where $A_p(z)$ are analytic functions in the neighborhood of $z=\mu(T,\sigma=0)\pm\mathcal{N}(T,\sigma=0)$. It thus follows trivially that both the nematic order parameter and the "mass" of the CDW fluctuations (which determines the longest CDW correlation length as shown in Eq. **S46**, below) are analytic functions of disorder strength:

$$\mu_-(T,\sigma)\equiv\mu(T,\sigma)-\left|\mathcal{N}(T,\sigma)\right|=\mu_-(T,0)+\mathcal{O}(\beta\sigma^2), \qquad \text{[S32]}$$

$$\left|\mathcal{N}(T,\sigma)\right|=\left|\mathcal{N}(T,0)\right|-\mathcal{O}(\beta\sigma^2)\quad\text{for}\quad T_{\text{str}}<T<T_{\text{nem}}. \qquad \text{[S33]}$$

Note that $\mathcal{N}$ is, by definition, the nematic order parameter and μ_- is a measure of how far the system is from a CDW ordered state—below, we relate it to the CDW correlation length.

For $T<T_{\text{str}}$, the analysis is a bit more subtle, because $\mu_-(T,\sigma)\to 0$ as $\sigma\to 0$. The results, moreover, depend on the asymptotic

forms of $A_p(\mu)$ at small μ. In $d=3$ the leading-order behavior as $z\to 0$ is readily derived from the asymptotic expressions

$$A_1(z)\sim A_1(0)-\left[\frac{A}{1-\alpha}\right]z^{1-\alpha}+\ldots \quad \text{and}$$
$$A_2(z)\sim Az^{-\alpha}+\ldots \quad \text{with} \qquad [S34]$$
$$\alpha=\frac{4-d}{2}=\frac{1}{2} \quad \text{and} \quad A^{-1}=2\pi\sqrt{\left[J^2-(J')^2\right]V_z},$$

from which it follows that Eq. **S33** is still satisfied, but with

$$\mu_-(T,\sigma)=(1-\alpha)\beta\sigma^2+\mathcal{O}(\beta^3\sigma^4) \quad \text{for} \quad \beta\sigma^2\ll T<T_{\text{str}}. \qquad [S35]$$

(Surprisingly, in the range of T and σ to which this applies, μ_- is a decreasing function of T—because a smaller μ_- implies a larger correlation length, this corresponds to a range of temperatures in which the correlation length decreases with decreasing T!) Manifestly, for fixed small σ, this expansion breaks down at low T, but similar asymptotic analysis can be applied in the limit of low T and small σ to obtain

$$\mu_-(T,\sigma)\sim\left(\frac{A\sigma^2}{\Lambda}\right)^{1/\alpha}+\ldots \quad \text{for} \quad T\ll\sigma\ll T_{\text{str}}, \qquad [S36]$$

$$\mathcal{N}\sim\Lambda\Delta-2TA_1(2\Lambda\Delta)-2\sigma^2A_2(2\Lambda\Delta)+\ldots, \qquad [S37]$$

where $\ldots$ signifies higher-order terms in both T and σ.

In a highly anisotropic system ($d\approx 2$), with $V_z\ll J$, there is an intermediate asymptotic regime in which $J\gg\beta\sigma^2\gg V_z\gg J/\xi_{2D}$, in which the asymptotic forms of A_p can be computed with $V_z=0$, in which case

$$A_1(z)\sim A\ln\left[\frac{J}{z}\right]+\ldots \quad \text{and}$$
$$A_2(z)\sim A\mu^{-1}+\ldots \quad \text{with} \qquad [S38]$$
$$A^{-1}=4\pi\sqrt{\left[J^2-(J')^2\right]}.$$

In this limit, as well, Eq. **S33** governs the evolution at small σ.

Altogether, independent of regime, the above analysis confirms, as shown in Fig. 1 in the main text, that the nematic order parameter is a continuous function of disorder, regardless of whether there is CDW order in the $\sigma\to 0$ limit.

Similar asymptotic analysis can be applied to determining the shape of the phase diagram. For small enough V_z, the nematic transition is continuous, so we can identify T_{nem} by equating the derivate with respect to $\mathcal{N}$ of the left and right sides of Eq. **S29**. The critical value $\mu_c\equiv\mu(T_{\text{nem}})$ is obtained as the solution of the implicit equation

$$\Lambda\Delta A_2(\mu_c)-A_1(\mu_c)=2\Delta\sigma^2\left[A_2^2(\mu_c)-2A_1(\mu_c)A_3(\mu_c)\right] \qquad [S39]$$

in terms of which

$$T_{\text{nem}}=\frac{\Lambda-2\sigma^2A_2(\mu_c)}{2A_1(\mu_c)}, \qquad [S40]$$

while breaking of $SO(N)$ symmetry is allowed in $d=3$ in the absence of disorder ($\sigma=0$), but not in the presence of disorder. Because μ_c is nonzero, all of the dependence of the saddle-point equations on $\mathcal{N}$ is analytic for small $\mathcal{N}$. Consequently, as in any other mean-field theory,

$$\mathcal{N}(T)\sim\mathcal{N}_0\sqrt{[T_{\text{nem}}-T]/T_{\text{nem}}} \qquad [S41]$$

for $T_{\text{nem}}\gg[T_{\text{nem}}-T]>0$. T_{nem} is a monotone decreasing function of σ such that

$$T_{\text{nem}}\to\frac{\Lambda}{2A_1(\mu_c)} \quad \text{as} \quad \sigma\to 0, \qquad [S42]$$

where μ_c is the solution of the implicit equation

$$\Delta\Lambda=\frac{A_1(\mu_c)}{A_2(\mu_c)} \qquad [S43]$$

and

$$T_{\text{nem}}\to 0 \quad \text{as} \quad \sigma^2\to\sigma_c^2=\frac{\Lambda}{[2A_2(\mu_0)]}, \qquad [S44]$$

where μ_0 is the solution of the implicit equation

$$2\Delta\Lambda=\frac{A_2(\mu_0)}{A_3(\mu_0)}. \qquad [S45]$$

Note that these equations have a nonzero solution for any nonzero Δ.

The phase diagram in Fig. 1 of the main text interpolates between these various asymptotic expressions and was obtained by solving the self-consistency equations numerically. Because we have focused on relatively small values of V_z, all of the transitions are continuous. For larger values of V_z, where in the clean limit there is a single first-order transition to a stripe-ordered phase (i.e., for V_z larger than the value at the critical end point in Fig. 1), the nematic transition in the weak disorder limit is also first order. We have not analyzed this limit extensively.

The CDW Structure Factor. The self-consistent fields, μ and $\mathcal{N}$, are the key quantities that determine the behavior of the response functions of the system, as well as its thermodynamic state. The CDW structure factor, $S(\mathbf{k})$ for $\mathbf{k}$ near the clean-limit ordering vectors, $Q\hat{x}$ and $Q\hat{y}$, is expressed in terms of the propagator, $G(\mathbf{k};\mu\pm\mathcal{N};\pm)$, in Eq. **S12**. The expected line shape consists of a sum of a Lorentzian and a squared Lorentzian. As a function of decreasing temperature, the relative weight of the two factors shifts from being dominated by the former at high T to being dominated by the latter at low T. From the width of the peaks, one can extract a set of CDW correlation lengths (expressed in units of the lattice constant, as is appropriate for the lattice model in Eq. **S2**—in terms of the original CDW, this lattice constant is a somewhat ill-defined ultraviolet cutoff that should be interpreted to be something like the CDW wavelength). In general, there is an in-plane longitudinal and transverse correlation length, ξ_L and ξ_T, as well as a correlation length in the z direction, ξ_z; in a nematic state, all these correlation lengths are different near the two ordering vectors. Specifically,

$$\xi_L(Q\hat{x})=\sqrt{\frac{(J+J')}{2(\mu-\mathcal{N})}}, \quad \xi_L(Q\hat{y})=\sqrt{\frac{(J+J')}{2(\mu+\mathcal{N})}}, \qquad [S46]$$

$$\xi_T(Q\hat{x})=\sqrt{\frac{(J-J')}{2(\mu-\mathcal{N})}}, \quad \xi_T(Q\hat{y})=\sqrt{\frac{(J-J')}{2(\mu+\mathcal{N})}}, \qquad [S47]$$

$$\xi_z(Q\hat{x})=\sqrt{\frac{V_z}{2(\mu-\mathcal{N})}}, \quad \xi_z(Q\hat{y})=\sqrt{\frac{V_z}{2(\mu+\mathcal{N})}}. \qquad [S48]$$

The maximum scattering intensity is even more directly related to the self-consistent fields,

$$S(Q\hat{x}) = \frac{T}{(\mu - \mathcal{N})} + \frac{\sigma^2}{(\mu - \mathcal{N})^2}, \quad S(Q\hat{y}) = \frac{T}{(\mu + \mathcal{N})} + \frac{\sigma^2}{(\mu + \mathcal{N})^2}. \tag{S49}$$

The integrated intensity in each of the two peaks is

$$I(Q\hat{x}) = \Lambda - I(Q\hat{y}) = TA_1(\mu - \mathcal{N}) + \sigma^2 A_2(\mu - \mathcal{N}). \tag{S50}$$

The nematic character of the state can, in principle, be seen in measures of the CDW structure factor as the difference between properties near $Q\hat{x}$ and $Q\hat{y}$. Where the CDW correlation length is long, so that $\mu + |\mathcal{N}| \gg \mu - |\mathcal{N}|$, this is straightforward. However, for relatively short CDW correlation lengths, where $\mu \gg |\mathcal{N}|$, the nematic character of the CDW state is relatively subtle. For instance, from Eq. **S49**,

$$\frac{S(Q\hat{x}) - S(Q\hat{y})}{S(Q\hat{x}) + S(Q\hat{y})} = \frac{\mathcal{N}}{\mu}\left(\frac{T\mu + 2\sigma^2}{T\mu + \sigma^2}\right) + \mathcal{O}\left(\frac{\mathcal{N}}{\mu}\right)^3. \tag{S51}$$

In Fig. S2 we exhibit the behavior of the correlation lengths as a function of T for various values of the parameters. These were obtained by numerically solving the saddle-point equations, Eq. **S31**. It is important to note, before comparing these to experiment, that these were computed assuming a constant (temperature-independent) Λ; in general, Λ (which sets the total amplitude of the CDW correlations) should be only weakly temperature dependent at temperatures small compared with the mean-field T_c, but is a strongly decreasing function of T at temperatures approaching the mean-field transition temperature. Indeed, this effect enhances the T dependences of all CDW-related correlations at elevated temperatures.

Subtleties and Higher-Order Effects

For the most part, we have focused on the primary order parameters in the problem and have treated explicitly only the lowest-order terms in a Landau–Ginzburg expansion in powers of the order parameter and its gradients. There are, however, some subtle pieces of qualitative physics that require higher-order terms or that require analyzing terms beyond saddle-point approximation (or equivalently, terms higher order in powers of $1/N$). Here we mention a few of these subtleties.

Structure at Harmonics of the Fundamental. In the absence of disorder, where there is long-range CDW order at one or more of the fundamental ordering vectors, $Q\hat{x}$ or $Q\hat{y}$, one generically expects peaks at harmonics as well, albeit they are generically weaker, as they are higher order in powers of the order parameter in the regime where the Landau–Ginzburg theory is applicable. Observation of these harmonics can be useful in distinguishing the nature of the charge-ordered state. For instance, if there is no way to obtain a macroscopic single-domain order, it may be difficult to distinguish stripe from checkerboard order by looking only at the fundamentals. [Sometimes, however, due to peculiarities of the crystal structure, even just looking at the fundamentals may be sufficient to distinguish these two cases, even in the presence of multiple domains (3).]

Specifically, in a stripe-ordered state in a tetragonal crystal with an equal number of macroscopic x and y directed domains, there would be equal strength δ-function peaks in the structure factor at $\mathbf{q} = Q\hat{x}$ and $\mathbf{q} = Q\hat{y}$, just as there would be for a checkerboard-ordered state. However, although both states would also exhibit weaker second harmonic peaks at $\mathbf{q} = 2Q\hat{x}$ and $\mathbf{q} = 2Q\hat{y}$, the checkerboard state would also exhibit a second harmonic peak at $\mathbf{q} = \mathbf{Q}_{xy} \equiv Q\hat{x} + Q\hat{y}$ that would be absent in the stripe-ordered state. So it is reasonable to ask whether the same is true of the not-quite-ordered CDW state in the presence of nonzero disorder.

The structure factor in the neighborhood of these second harmonics is the Fourier transform of the correlation functions of the bilinear order parameter, $\tilde{S}_{\alpha\alpha'}(\mathbf{r})$. In the $U(1)$ representation, where ψ_α is a complex scalar field, the second harmonic is also a complex scalar field, $\psi_{\alpha\alpha'} = \psi_\alpha \psi'_\alpha$, which transforms under translations as $\psi_{\alpha\alpha'} \to e^{iQ(r_\alpha + r_{\alpha'})}\psi_{\alpha\alpha'}$. In the $O(2)$ representation, where $\psi_{i\alpha}$ is a real vector field with $\psi_{1\alpha} = \mathrm{Re}[\psi_\alpha]$ and $\psi_{2\alpha} = \mathrm{Im}[\psi_\alpha]$, the same composition law [written in a way that is straightforward to generalize to $SO(N)$] is (adopting summation convention)

$$\psi_{\alpha\alpha';jj'}(\vec{r}, m) = \frac{g_2}{N}\psi_{\alpha,i}(\vec{r}, m)\Gamma^{(jj')}_{i,i'}\psi_{\alpha',i'}(\vec{r}, m), \tag{S52}$$

where Γ are the traceless symmetric tensors,

$$\Gamma^{(ij)}_{kp} = \Gamma^{(ij)}_{pk} = \Gamma^{(ji)}_{pk} = \delta_{ik}\delta_{jp} + \delta_{ip}\delta_{jk} - \frac{2}{N}\delta_{ij}\delta_{pk}, \tag{S53}$$

such that

$$\Gamma^{(ij)}_{pk}\Gamma^{(ij)}_{p'k'} = 2\Gamma^{(pk)}_{p'k'}. \tag{S54}$$

In terms of these,

$$\tilde{S}_{xy}(\vec{r}, m) = \sum_{ij} \overline{\left\langle \psi_{xy;ij}(\vec{r}, m)\psi_{xy;ij}(\vec{0}, 0)\right\rangle} \tag{S55}$$

and similarly for $\tilde{S}_{xx}$ and $\tilde{S}_{yy}$.

To lowest order in $1/N$, this means that the second harmonic structure factor is simply a convolution of the primaries, as in Eq. **12** in the main text. This expression has no explicit dependence on Δ and so does not depend any more sensitively than do the fundamentals on the sign of Δ (which would determine whether stripes or checkerboards were favored in the absence of disorder). The first correction that brings in an explicit dependence on Δ gives

$$\begin{aligned} S_{\alpha\alpha'}(\mathbf{k}) = {} & 2(g_2)^2\left[1 + \delta_{\alpha\alpha'} - \frac{2\delta_{\alpha\alpha'}}{N}\right]\prod_{\alpha\alpha'}(\mathbf{k}) \\ & - \frac{4(g_2)^2}{N}\int_q\int_{q'} S_\alpha(\mathbf{k}+\mathbf{q})S_{\alpha'}(\mathbf{q})V_{\alpha\alpha'}(\mathbf{q}-\mathbf{q}') \\ & \times S_\alpha(\mathbf{k}+\mathbf{q}')S_{\alpha'}(\mathbf{q}') + \mathcal{O}(N^{-2}), \end{aligned} \tag{S56}$$

where

$$\begin{aligned} V_{xy}(\mathbf{k}) &= 2D(\mathbf{k})^{-1}[U + \Delta] \\ V_{xx}(\mathbf{k}) &= 2D(\mathbf{k})^{-1}\left[(U - \Delta) - 4U\Delta\prod_{yy}(\mathbf{k})\right] \\ V_{yy}(\mathbf{k}) &= 2D(\mathbf{k})^{-1}\left[(U - \Delta) - 4U\Delta\prod_{xx}(\mathbf{k})\right] \\ D(\mathbf{k}) &= 1 + 2(U - \Delta)\left[\prod_{xx}(\mathbf{k}) + \prod_{yy}(\mathbf{k})\right] \\ & \quad - 8U\Delta\prod_{xx}(\mathbf{k})\prod_{yy}(\mathbf{k}) \end{aligned} \tag{S57}$$

and where

$$\prod_{\alpha\alpha'}(\mathbf{k}) = \int \frac{d^3q}{(2\pi)^3} S_\alpha(\mathbf{q})S_{\alpha'}(\mathbf{k}+\mathbf{q}). \tag{S58}$$

This is a complicated expression, but the qualitative point can be seen directly: The leading-order term contains no additional information to distinguish stripe and checkerboard orders that is not already apparent in the structure factor near the fundamental ordering vectors. The first $1/N$ correction is generally negative; i.e., it tends to suppress the magnitude of the harmonic peaks, but it does depend explicitly on the sign of Δ. In particular, for positive Δ, the structures at $2Q\hat{x}$ and $2Q\hat{y}$ are suppressed less than the structure at $\mathbf{Q}_{xy}$, whereas negative Δ has the opposite effect.

The expression can be somewhat simplified in the hard-spin limit $U \to \infty$, where

$$\begin{aligned} V_{xy} &\to \left[\Pi_{xx} + \Pi_{yy} - 4\Delta \Pi_{xx}\Pi_{yy}\right]^{-1} \\ V_{xx} &\to V_{xy}\left[1 - 4\Delta\Pi_{yy}\right] \\ V_{yy} &\to V_{xy}\left[1 - 4\Delta\Pi_{xx}\right]. \end{aligned} \qquad \text{[S59]}$$

Here the qualitative response to the sign of Δ is apparent. However, it is clear that unless there is a very pronounced peak at the harmonic ordering vector (so that $\Delta S_{\alpha\alpha}$ is significant), such effects will be subtle and difficult to interpret.

Shifts of the Ordering Vector. One unphysical feature of the model we have treated is that the ordering wave vector is constant, independent of T and σ and any of the other variables. In contrast, incommensurate density waves generically have T-dependent ordering vectors. This can be corrected by including higher-order terms in the effective field theory—of which the lowest-order terms are

$$\begin{aligned} \delta\mathcal{H} = &\frac{g_+}{iN}\left[|\psi_x|^2 + |\psi_y|^2 - N\Lambda\right]\left[\psi_x^\dagger \partial_x \psi_x + \psi_y^\dagger \partial_y \psi_y\right] \\ &+ \frac{g_-}{iN}\left[|\psi_x|^2 - |\psi_y|^2\right]\left[\psi_x^\dagger \partial_x \psi_x - \psi_y^\dagger \partial_y \psi_y\right] + \ldots \end{aligned} \qquad \text{[S60]}$$

At first blush, these terms appear to violate inversion symmetry, but it is important to recall that zero momentum in the effective field theory actually corresponds to momentum $Q\hat{e}_\alpha$ in physical terms. Thus, positive momenta add to Q whereas negative momenta reduce it in magnitude.

The first term here produces a generally T- and σ-dependent shift in the magnitude of the ordering vector, but it vanishes in the hard-spin limit. There still may be some smooth T dependence of Q, which comes from high-energy physics and appears as an analytic temperature dependence of Q that can be included explicitly, but does not reflect any of the emergent physics of a growing CDW correlation length.

The second term is significant in the nematic phase, where it produces a relative shift between the ordering vectors in the x and y, which to leading order in $1/N$ is

$$\delta\mathbf{Q}_x = \left(\frac{\mathcal{N}}{2\Delta\kappa_\parallel}\right)\hat{x} \quad \text{and} \quad \delta\mathbf{Q}_y = -\left(\frac{\mathcal{N}}{2\Delta\kappa_\parallel}\right)\hat{y}. \qquad \text{[S61]}$$

Coupling to Strain. A major difference between $\mathbf{Q} = \mathbf{0}$ and nonzero orders is the implications of their coupling to strain: For nonzero $\mathbf{Q}$, the induced interactions fall exponentially with distance, and so if the coupling to the lattice is weak, the effects are negligible. By contrast, for $\mathbf{Q} = \mathbf{0}$ order, including nematicity, strain-induced effective interactions are long ranged and hence can have important consequences even if weak. One particularly important consequence of this is that even if the electronic structure is quasi-2D (i.e., $V_z \ll J$), so that the CDW correlations are essentially confined to single planes, the interplane nematic couplings can nonetheless be significant. Such strain effects first appear in the effective field theory through terms of the form

$$\delta\mathcal{H} = \ldots + g_{\text{strain}}\left[\epsilon_{xx} - \epsilon_{yy}\right]\left[\psi_x^\dagger \psi_x - \psi_y^\dagger \psi_y\right] + \ldots, \qquad \text{[S62]}$$

where $\epsilon_{\alpha\alpha'}$ is the strain tensor. Not coincidently, this term also embodies the coupling of the nematic order to any small orthorhombicity of the crystal, where in this case $\epsilon_{\alpha\alpha'}$ is the orthorhombic strain defined relative to a putative tetragonal parent compound.

Are the CDW Sightings in the Different Hole-Doped Cuprates Closely Related?

There has been some debate about whether the CDW tendencies seen in the various different cuprates are close siblings or many-times removed cousins—i.e., whether the differences from one family of cuprates to another are the expected "small" effects produced by the somewhat different crystalline environment and degree of quenched disorder in the different materials or are so "large" that they should be thought of as different phenomena with different mechanisms. This latter viewpoint seems untenable to us, for reasons that are elaborated elsewhere (4, 5).

It is, however, worth mentioning that there is very compelling evidence from transport that the basic charge-ordering phenomena are extremely closely related in all of the families of hole-doped cuprates. Specifically, several transport signatures of the incipient charge order have been identified by Taillefer and coworkers (6–9) by studying various stripe-ordered 214 materials, including LBCO, NdLSCO, and EuLSCO. Because the CDW order has particularly long correlation lengths in these materials (and hence is easier to identify in scattering experiments), they were able to correlate the diffraction data with salient features of the transport data. This identification is significant in its own right—it shows that the CDW ordering phenomena have a significant effect on the low-energy itinerant electronic structure, i.e., that it is an "important" actor in the electronic physics of these materials.

Taillefer and coworkers then measured the same transport properties in YBCO and Hg1201 in the same range of copings and saw extraordinarily similar features. In some cases, transport data (8, 9) from NdLSCO, YBCO, and Hg1201 at the same doping can be laid on top of each other and are essentially indistinguishable. (The CDW transition in LBCO is sharper than in the other materials, as reflected in its longer correlation length, and correspondingly the associated features in the transport are anomalously sharp in this material.) It is difficult to imagine that there could be significant differences in the nature of the charge ordering in the different families of hole-doped cuprates, given the great similarities between the transport signatures.

1. Tarjus G, Tissier M (2008) Nonperturbative functional renormalization group for random field models and related disordered systems. I. Effective average action formalism. *Phys Rev B* 78(2):024203(1)–024203(19).
2. Amit DJ (1984) *Statistical Field Theory* (World Scientific, Singapore).
3. Robertson JA, et al. (2006) Distinguishing patterns of charge order: Stripes or checkerboards. *Phys Rev B* 74(13):134507(1)–134507(10).
4. Fradkin E, Kivelson SA (2012) High-temperature superconductivity: Ineluctable complexity. *Nat Phys* 8:864–866.
5. da Silva Neto EH, et al. (2014) Ubiquitous interplay between charge ordering and high-temperature superconductivity in cuprates. *Science* 343(6169):393–396.
6. Doiron-Leyraud N, Taillefer L (2012) Quantum critical point for stripe order: An organizing principle of cuprate superconductivity. *Physica C* 481:161–167.
7. Chang J, et al. (2010) Nernst and Seebeck coefficients of the cuprate superconductor $YBa_2Cu_3O_{6.67}$: A study of Fermi surface reconstruction. *Phys Rev Lett* 104(5):057005.
8. Laliberté F, et al. (2011) Fermi-surface reconstruction by stripe order in cuprate superconductors. *Nat Commun* 2:432.
9. Doiron-Leyraud N, et al. (2013) Hall, Seebeck, and Nernst coefficients of underdoped $HgBa_2CuO_{4+\delta}$: Fermi-surface reconstruction in an archetypal cuprate superconductor. *Phys Rev X* 3(2):021019(1)–021019(7).

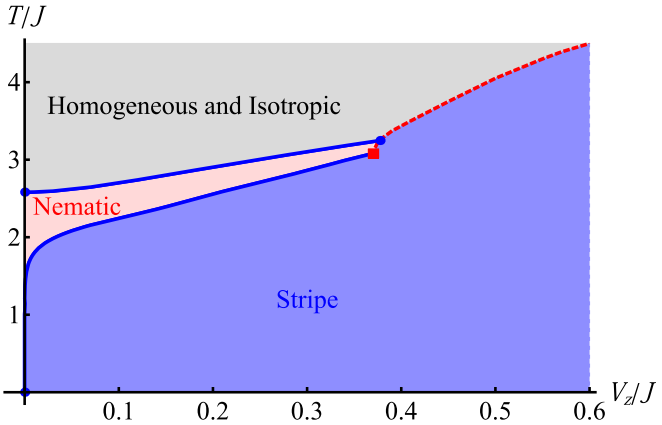

Fig. S1. The phase diagram in the clean limit ($\sigma = 0$) as a function of T and interplane coupling, V_z, with $J = 1, J' = 0.01$, and $\Delta = 0.25$ obtained by numerically solving Eq. **S31**. The solid and dashed lines represent, respectively, continuous and first-order phase transitions, the square shows a classical tricritical point, and the solid circle shows a critical end point. The phase boundary of the stripe phase has been shifted, for graphical clarity, because the nematic phase typically is confined to a still narrower range of T than shown.

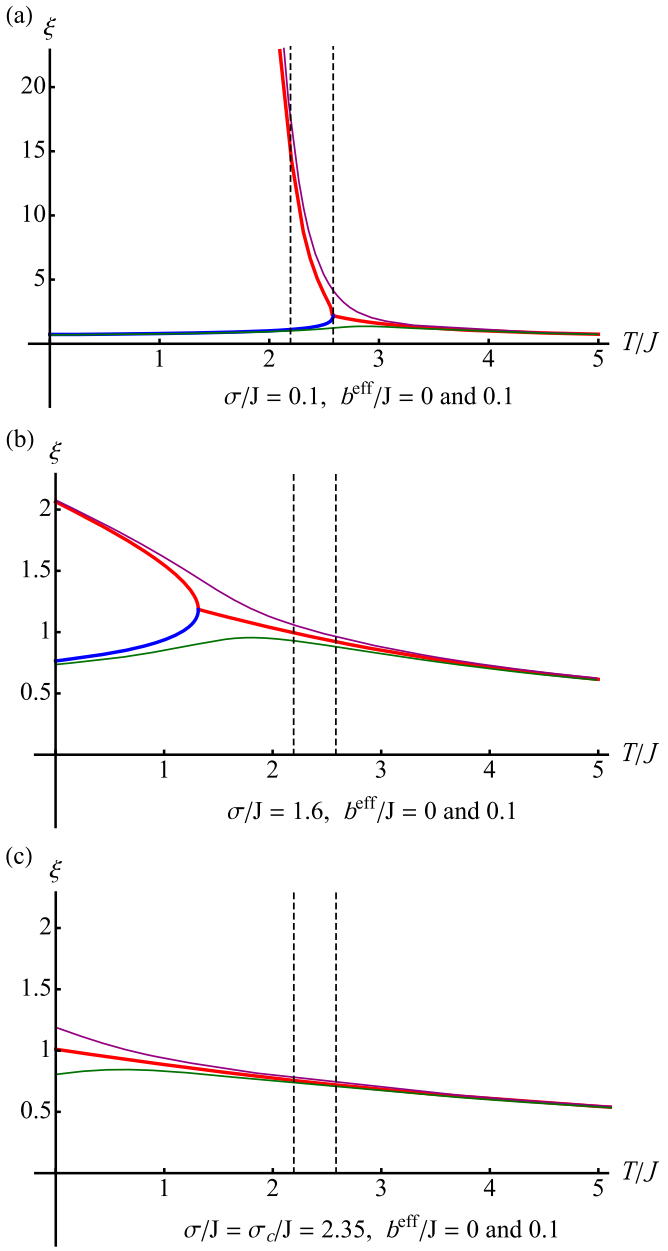

Fig. S2. (*A*–*C*) *T* dependence of correlation lengths from the solution of Eq. **S31** for various disorder strengths and in the presence or absence of explicit symmetry breaking. Here $J = 1, J' = 0.01, V_z = 0.01, \Delta = 0.25$, and ξ is the correlation length of ψ_α for $\alpha = x$ and y (upper and lower curves, respectively) in units of the lattice constant. (Because we have taken $J' \ll J$, there is little difference between the transverse and longitudinal correlation lengths.) The clean-limit stripe and nematic transition temperatures are $T_{str} = 2.19J$ and $T_{nem} = 2.58J$, respectively, represented by dashed lines in *A*–*C*. Thick lines are computed for $b^{eff} = 0$ whereas for the thin lines there is an explicit symmetry-breaking field $b^{eff} = 0.1J$. The critical disorder strength above which there is no nematic transition is $\sigma_c = 2.35J$. Note that the lattice constant of the effective spin model was introduced to provide an ultraviolet regularization of the theory—physically, it should be roughly associated with the larger of the CDW period or the CDW mean-field (amplitude) coherence length.